

FEASIBILITY OF SINGLE-SHOT MICROBUNCHING DIAGNOSTICS FOR A PRE-BUNCHED BEAM AT 266 nm*

A. H. Lumpkin^{#1} and D.W. Rule²

¹Argonne Associate, Argonne National Laboratory, Lemont, IL, USA

²Silver Spring, MD, USA

Abstract

We describe potential characterization of microbunched electron beams obtained after a modulator and chicane by using coherent optical transition radiation (COTR) imaging techniques. Beam transverse size (~50 microns), divergence (sub-mrad), trajectory angle (within ~0.1 mrad), spectrum (to a few nm), and pulse length (sub-ps) can be measured. The transverse spatial alignment is provided with near-field imaging, and the angular alignment is done with far-field imaging and two-foil COTR interferometry (COTRI). Analytical model results for a 266-nm wavelength COTRI case with a 10% microbunching fraction will be presented. COTR gains of 7×10^6 were calculated for an initial charge of 300 pC, and this enables splitting the optical signal for single-shot measurements of all the cited parameters.

INTRODUCTION

Co-propagating a relativistic electron beam and a high-power laser pulse through a short undulator (modulator) provides an energy modulation which can be converted to a periodic longitudinal density modulation (or microbunching) via the R56 term of a chicane [1]. Such pre-bunching of a beam at the resonant wavelength and the harmonics of a subsequent free-electron laser (FEL) amplifier seeds the process and results in improved gain. We describe potential characterizations of the resulting microbunched electron beams after the modulator using coherent optical transition radiation (COTR) imaging techniques for transverse size (50 micron), divergence (sub-mrad), trajectory angle (0.1 mrad), spectrum (few nm), and pulse length (sub-ps). The transverse spatial alignment is provided with near-field imaging and the angular alignment is done with far-field imaging and two-foil COTR interferometry (COTRI). Analytical model results for a 266-nm wavelength COTRI case with a 10% microbunching fraction will be presented. COTR gains of 7 million were calculated for an initial charge of 300 pC which enables splitting the optical signal for single-shot measurements of all the cited parameters. Since the beam and laser position jitters may cause some fluctuations in the microbunching spatial distribution, single-shot diagnostics will be beneficial.

*Work supported under Contract No. DE-AC02-07CH11359 with the United States Department of Energy, Basic Energy Sciences.
#lumpkin@anl.gov

EXPERIMENTAL ASPECTS

The APS Linac

The APS linac is based on an S-band rf photocathode (PC) gun which injects beam into an S-band linear accelerator with acceleration capability up to 450 MeV [2]. Beam diagnostics include imaging screens, rf BPMs, and coherent transition radiation (CTR) autocorrelators located before and after the chicane at the 100 MeV point.

The Microbunching Diagnostics

The diagnostics for the microbunching experiments would be located in the linac extension area (LEA) [2]. A schematic of a potential setup is shown in Fig. 1. A seed laser at 266 nm would be injected onto the beamline axis at a chicane to co-propagate with a 375-MeV electron beam micropulse through a modulator section. Immediately after the modulator, a set of 4 magnets would provide a small dispersive, R56 term to convert the energy modulation to the longitudinal density modulation. Such an electron beam would be transported to the COTR diagnostics. As will be shown later, the COTR gain will be significant at 6 orders of magnitude over incoherent OTR so the signal can be split over multiple optical paths for near field (NF) imaging, far-field (FF) imaging, spectral measurements, gain measurements, and a bunch length measurement with a streak camera. A thin laser blocking foil will be inserted before a mirror at 45 degrees to the beam direction as indicated in Fig. 1. A microscope objective will be focused on the back surface of the foil for the forward COTR beam size to provide a NF image in one UV camera. The combination of this source and the backward COTR from the mirror will result in interference fringes when viewed in the far field by a second UV camera. The enhanced light may also be split to provide signals to a UV-visible spectrometer (also readout by a UV camera) and a UV-visible streak camera. We may utilize a C5680 Hamamatsu streak camera with S20 PC operating with the M5675 synchroscan vertical deflection unit phase locked to 119.0 MHz, the 24th subharmonic of the linac S-Band at 2856 MHz. As will be noted in a subsequent section, a unique beam-based alignment technique will be employed using the COTR and COTRI images. The shape and intensity of the images at 266 nm will provide immediate online information on the overlap of the seed laser and e-beam, both spatially and temporally.

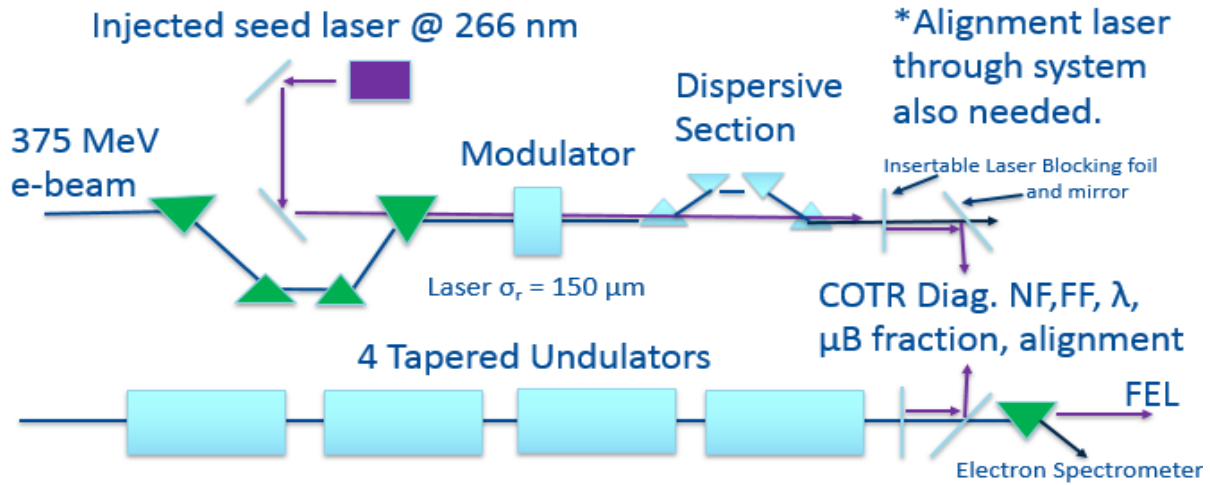


Figure 1: Schematic of the proposed LEA beamline layout showing the chicane, injected seed laser, modulator, COTR screens, undulators, and electron spectrometer.

ANALYTICAL MODEL AND RESULTS

Optical Transition Radiation Basics

When a charged-particle beam transits the interface of two different media, optical transition radiation (OTR) is generated by induced currents at the boundary of those media with different dielectric constants. As schematically shown in Fig. 2, there are forward and backward radiation cones emitted with opening angle of $1/\gamma$ (where γ is the relativistic Lorentz factor) around the angle of specular reflection for the backward OTR and around the beam direction for the forward OTR. For a nominal case of 375 MeV, a foil separation $L=6.3$ cm, a wavelength of 266 nm, and a beam divergence of 0.1 mrad, one obtains the two-foil angular distribution pattern (red curve) as shown in Fig. 3, which is compared to the single foil pattern (black curve). The fringe visibility decreases with larger divergence values, and this dependence then can be used for a divergence measurement.

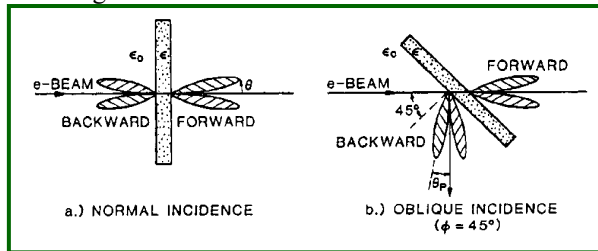


Figure 2: Schematic of OTR generation at boundaries of vacuum and materials for a) normal incidence and b) oblique incidence [3].

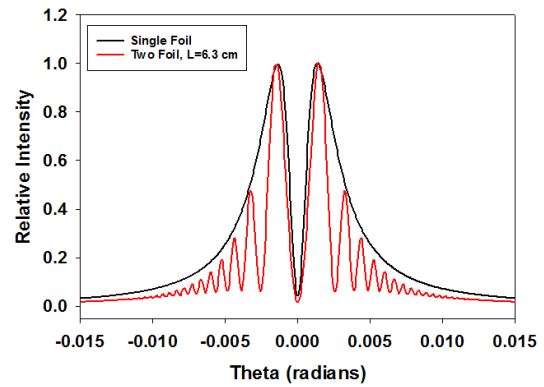


Figure 3: Comparison of far field OTR angular distribution patterns for a single foil and a two-foil interferometer. A beam energy of 375 MeV, wavelength of 266 nm, $L=6.3$ cm, and a divergence of $\sigma_\theta = 0.1$ mrad were used in the calculations.

The number W_1 of OTR photons that a single electron generates per unit frequency ω per unit solid angle Ω is

$$\frac{d^2W_1}{d\omega d\Omega} = \frac{e^2}{\hbar c} \frac{1}{\pi^2 \omega} \frac{(\theta_x^2 + \theta_y^2)}{(\gamma^{-2} + \theta_x^2 + \theta_y^2)^2} \quad (1)$$

where \hbar is Planck's constant/ 2π , e is the electron charge, c is the speed of light, and θ_x and θ_y are radiation angles [4].

COTRI Model Results at 266 nm

The addition of the interference term $I(\mathbf{k})$ and the coherence function $J(\mathbf{k})$ as shown in Eqs. 2-5 include the effects of the microbunched fraction $f_B=N_B/N$, N_B being the microbunched part of the total N .

$$\frac{d^2W}{d\omega d\Omega} = |r_{\parallel,\perp}|^2 \frac{d^2W_1}{d\omega d\Omega} I(\mathbf{k})J(\mathbf{k}) \quad (2)$$

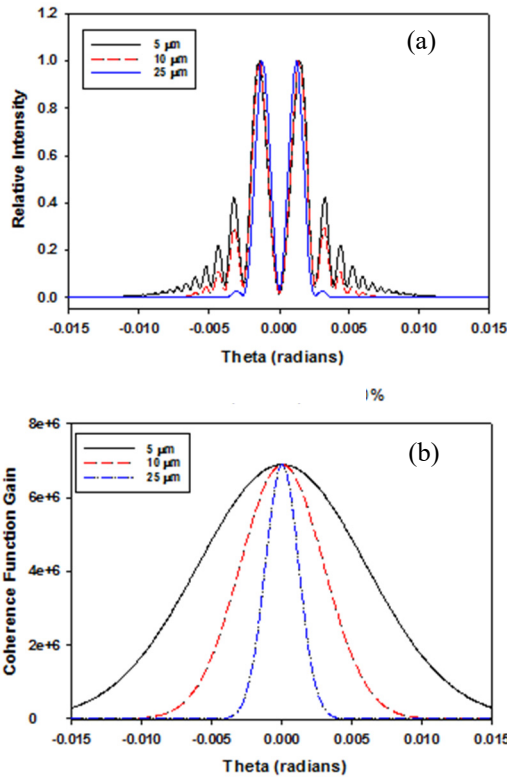


Figure 4: COTRI calculations for a) fringes and b) coherence function for beam sizes of 5, 10, and 25 μm .

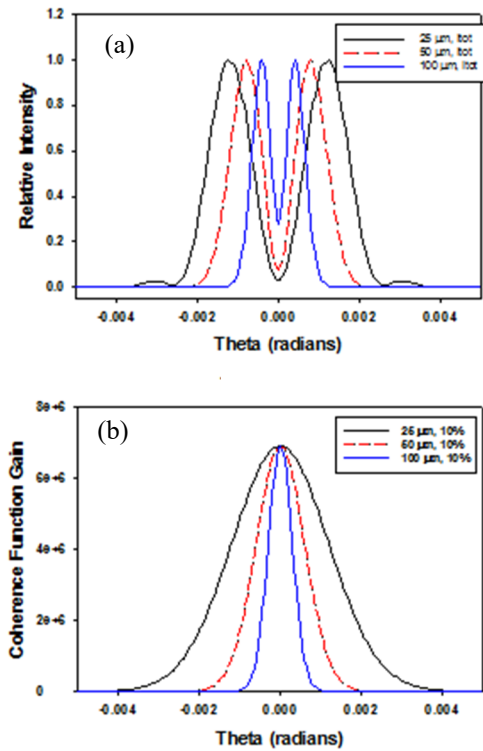


Figure 5: COTRI calculations for (a) fringes and (b) coherence function for beam sizes of 25, 50, and 100 μm .

$$I(\mathbf{k}) = 4 \sin^2 \left[\frac{kL}{4} (\gamma^{-2} + \theta_x^2 + \theta_y^2) \right] \quad (3)$$

$$J(\mathbf{k}) = N + N_B(N_B - 1) |H(\mathbf{k})|^2 \quad (4)$$

$$H(\mathbf{k}) = \frac{\rho(\mathbf{k})}{q} = g_x(k_x) g_y(k_y) F_z(k_z) \quad (5)$$

where $H(\mathbf{k})$ is the Fourier transform of the charge form factors for a single microbunch [4].

The COTRI calculations with the same parameters as Fig. 3 except with $N_B > 0$, for 5, 10 and 25 μm beam sizes show the effect of the microbunched transverse size on the coherence function as a function of angle in Fig 4a. The smallest beams result in the largest angles over which fringes are enhanced. The maximum enhancement is on axis at zero radians in Fig. 4b and shows a gain of 7×10^6 for this case of $f_B = 0.10$ microbunching fraction with 300 pC micropulse charge.

In Figure 5 similar plots are done for 25, 50 and 100 μm , and a noticeable loss of the outer fringe enhancements for these larger beam sizes is observed in Fig. 5a. Note, the angular range plotted is much smaller than that in Fig. 4, but the gain at zero mrad is still 7 million in Fig. 5b.

Angular Alignment Example

These angular distribution patterns can also be used for beam-based angular alignment of the seed laser and the electron beam. The proof of concept is shown in Fig. 6 for the case of the overlap of the SASE FEL beam and the electron beam [5]. Initially, we observed the asymmetric COTRI lobe pattern after undulator 8. By using a steering corrector before undulator 8, we were able to steer for symmetry in the lobes of the image. As a result, we improved the FEL gain by ~ 3.7 times through this one undulator section over the as-found state using rf BPMs and intensities of SASE FEL output as a function of z .

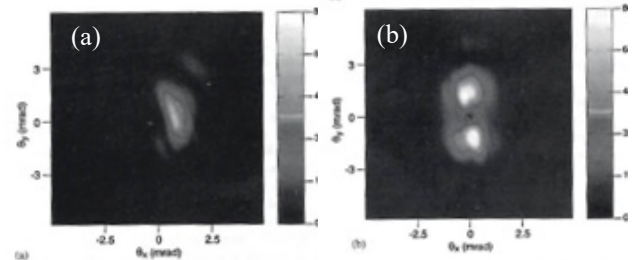


Figure 6: COTRI FF Image at 540 nm obtained after Undulator #8 in previous SASE FEL setup before (a) and after (b) corrected steering [5].

SUMMARY

In summary, we have evaluated the potential of using COTRI-based diagnostics to obtain single-shot characterizations of the transverse beam properties of microbunched electrons from a pre-buncher configuration at 266 nm. The spatial and temporal overlap aspects of the laser pulse and electron micropulse can in principle be addressed as well in an online manner.

ACKNOWLEDGMENTS

The first author acknowledges the support of J. Byrd and discussions with A. Zholents, both at Argonne National Laboratory.

REFERENCES

- [1] L.-H. Yu, "Generation of intense uv radiation by subharmonically seeded single-pass free-electron lasers", *Phys. Rev. Lett. A*, vol. 44, p. 5178, 1991.
doi: 10.1103/PhysRevA.44.5178
- [2] Y. Sun *et al.*, "APS LINAC Interleaving Operation", in *Proc. 10th Int. Particle Accelerator Conf. (IPAC'19)*, Melbourne, Australia, May 2019, pp. 1161-1163.
doi:10.18429/JACoW-IPAC2019-MOPTS119
- [3] A. H. Lumpkin, *Accel. Instr. Workshop*, Batavia IL, AIP Conf. Proc., vol. 229, p. 151, 1991.
- [4] D. W. Rule and A. H. Lumpkin, "Analysis of Coherent Optical Transition Radiation Interference Patterns Produced by SASE-Induced Microbunches", in *Proc. 19th Particle Accelerator Conf. (PAC'01)*, Chicago, IL, USA, Jun. 2001, paper TPAH029, pp. 1288-1290.
- [5] A. H. Lumpkin *et al.*, "On-line SASE FEL gain optimization using COTRI imaging", *Nuclear Instruments and Methods in Physics Research Section A*, vol. 528, p. 179, 2004.
doi:10.1016/j.nima.2004.04.042